International Journal of Nanomedicine

Dovepress
open access to scientific and medical research

Open Access Full Text Article

ORIGINAL RESEARCH

A Contrast Examination of Proinflammatory Effects on Kidney Function for γ-Fe_2O_3 NP and Gadolinium Dimeglumine

This article was published in the following Dove Press journal:
International Journal of Nanomedicine

Qian Xie[1,*]
Tao Wen[2,*]
Aiyun Yang[2]
Xue Zhang[2]
Bo Chen[3]
Jie Meng[2]
Jian Liu[2]
Ning Gu[4]
Haiyan Xu[2]

[1]Division of Nephrology, Peking University Third Hospital, Beijing, 100191, People's Republic of China; [2]Institute of Basic Medical Sciences Chinese Academy of Medical Sciences, School of Basic Medicine Peking Union Medical College, Beijing, 100005, People's Republic of China; [3]Materials Science and Devices Institute, Suzhou University of Science and Technology, Suzhou, 215009, People's Republic of China; [4]State Key Laboratory of Bioelectronics, Jiangsu Key Laboratory for Biomaterials and Devices, School of Biological Science and Medical Engineering, Southeast University, Nanjing, 210096, People's Republic of China

*These authors contributed equally to this work

Correspondence: Haiyan Xu
Institute of Basic Medical Sciences Chinese Academy of Medical Sciences, School of Basic Medicine Peking Union Medical College, Beijing, 100005, People's Republic of China
Email xuhy@pumc.edu.cn

Ning Gu
State Key Laboratory of Bioelectronics, Jiangsu Key Laboratory for Biomaterials and Devices, School of Biological Science and Medical Engineering, Southeast University, Nanjing, 210096, People's Republic of China
Email guning@seu.edu.cn

Background: Contrast-enhanced magnetic resonance imaging (MRI) is a powerful diagnostic tool for many diseases. In many situations, the contrasts are repeatedly administrated in order to monitor and assess the disease progression.

Objective: To investigate and compare the biological effects of γ-Fe_2O_3 nanoparticle (NP) and gadolinium dimeglumine (Gd-DTPA) with high and multiple doses on the kidney of healthy mice.

Methods: Polydextrose sorbitol carboxymethyl ether coated γ-Fe_2O_3 NP with hydrodynamic size of 68.2 nm and clinically applied Gd-DTPA were employed on healthy mice with the repeatedly intravenous administration of high doses. The cell viability of human umbilical vein endothelial cells (HUVEC) in high doses of these two contrast agents were measured using the xCELLigence Real-Time Cell Analysis (RTCA) S16 Instrument. The biological effects of γ-Fe_2O_3 NP and Gd-DTPA on the kidney were obtained using a biochemical automatic analyzer and multiple proinflammatory factor kit on the serum. Histopathological and immunohistochemistry analysis were taken on kidney tissues.

Results: It showed that the proinflammatory responses elicited by the γ-Fe_2O_3 NPs were weaker than that by Gd-DTPA, evidenced by the relatively much lower level of IL-1β, IL-6, IL-18, TNF-α, C-reactive protein (CRP) and Ferritin. At the same time, the γ-Fe_2O_3 NPs did not have the biochemical index elevated, while the Gd-DTPA did.

Conclusion: The γ-Fe_2O_3 NPs induced weaker proinflammatory effects in reference to the Gd-DTPA, indicating better renal safety. Therefore, it is suggested that γ-Fe_2O_3 NPs should be safer and optional choice when repeated contrast-enhanced MRI is necessary.

Keywords: iron oxide nanoparticles, proinflammatory, cytokines, renal function

Introduction

Contrast-enhanced magnetic resonance imaging (MRI) is a common and necessary tool that has been used clinically for diagnosis of various organ diseases, such as cancer, infections, or bleeding.[1] In the process of imaging, contrast agents are usually administrated intravenously to enhance the visualization of illness lesions. Gadolinium (Gd)-based contrast agents (GBCAs) are currently the mainstream clinical MRI contrast agents.[2] However, there have been concerns on the increasing toxicological risk of nephrogenic systemic fibrosis (NSF) in patients with advanced renal dysfunction,[3] hence, GBCAs have been warned by the US Food and Drug Administration (FDA) to use in the patients with impaired renal function since 2010.[4]

Therefore, for patients with renal dysfunction, an optional MRI contrast agent is necessary. Iron oxide nanoparticles (NPs) have attracted lots of research interests due to their influence on relaxation time,[5–8] and still being largely investigated in nanomedicine including the cell targeting, labeling and separation, drug or gene delivery system, and hyperthermia.[9–14] There are two products of iron oxide NPs, namely ferumoxsil (Lumirems/Gastromarks) for oral administration and ferumoxide (Endorems/Feridexs) for intravenous injection received FDA approval previously, but both were discontinued for economic and safety issues reasons,[15–18] resulting from not adequate understanding of the drugs' action mechanisms.[19] So far there is one drug of Fe_3O_4 NPs, namely Ferumoxytol approved by the FDA for the treatment of iron deficiency anemia in chronic kidney disease though a warning about the risk of allergic reaction of this drug.[20] It can be noticed that this drug is off-label used when MRI enhancing images are required for patients suffering from various tumors or kidney transplants,[21] implying valuable potentials of the iron oxide NPs in MRI imaging for patients with renal diseases. Of note, differences between GBCAs and iron oxide NPs are not investigated adequately yet, especially the biological effects on the kidney in the context of repeated administration that is often required in clinical practices. For examples, researchers compared the interactions of one single injection of GBCAs and PEG coated small-sized γ-Fe_2O_3 NP in the healthy mice, examining the biodistribution and effects on the liver function, suggesting the iron oxide NP had a better safety profile than the GBCAs;[22] and another group studied the two contrasts in a renal failure rat model, showing the DSPE-PEG coated γ-Fe_2O_3 NP potentially could serve as an alternative to GBCAs in patients with renal diseases.[23] It has been noticed that the repeat exposure with GBCAs demonstrated the accumulation in organs, alerting a potential threat by repeating administration,[24] however, effects of repeat administration of GBCAs and iron oxide NP on the function of kidney are still an open question. The aim of this work is to compare the influence of polydextrose sorbitol carboxymethyl ether coated γ-Fe_2O_3 NP with hydrodynamic size of 68.2 nm and clinically applied GBCA gadolinium dimeglumine (Gd-DTPA), using the repeated administration regime and focusing on the long-term effects on the kidney from the aspect of inflammation in the level of both tissues and serum (Scheme 1).

This study was designed according to following reasons: first, as a regular diagnosis method, MRI may be conducted repeatedly every few months or weeks to assess the progress of disease or therapeutic efficacy for one patient. Second, although Gd-DTPA are considered safe for patients with normal kidney function, there are still several cases of Gd retention and fibrotic reactions reported,[25–27] strongly suggesting the Gd may trigger kidney injury in normal kidney for some populations. Here we showed that the serum kidney function indicators (BUN, Scr, and Cys-C) and blood inflammation factors (IL-1β, IL-6, IL-18, TNF-α, CRP and ferritin) of Gd-DTPA group were increased significantly when compared with those of γ-Fe_2O_3 NP and the control group. The histopathological analysis of the mice kidneys also indicated that γ-Fe_2O_3 NP was safer than Gd-DTPA with the repeatedly intravenous administration of high doses.

Materials and Methods

Reagents

Gd-DTPA was purchased from Bayer Pharma AG (Germany). Polydextrose sorbitol carboxymethyl ether coated iron oxide NPs (γ-Fe_2O_3 NPs) were synthetized by alternating-current magnetic field inducing method following the reference.[28] Stroke-physiological saline solution was purchased from Peking Union Medical College Hospital.

Characterizations

The morphology of γ-Fe_2O_3 NP was observed by transmission electron microscope (JEOL JEM-2100). Elemental analysis was performed with energy-dispersive X-ray (EDX) on field emission scanning electron microscope (FESEM, Hitachi S-4800, Tokyo, Japan). The hydrodynamic diameters and Zeta potential of γ-Fe_2O_3 NP were detected by a Zetasizer Nano ZS90 analyzer (Malvern instruments).

Cell Culture

Primary human umbilical vein endothelial cells (HUVECs) and endothelial cell medium were all purchased from ScienCell Research Laboratories (San Diego, CA). Cells were grown on a cell culture plates and cultured at 37°C in a wet incubator with 5% CO_2.

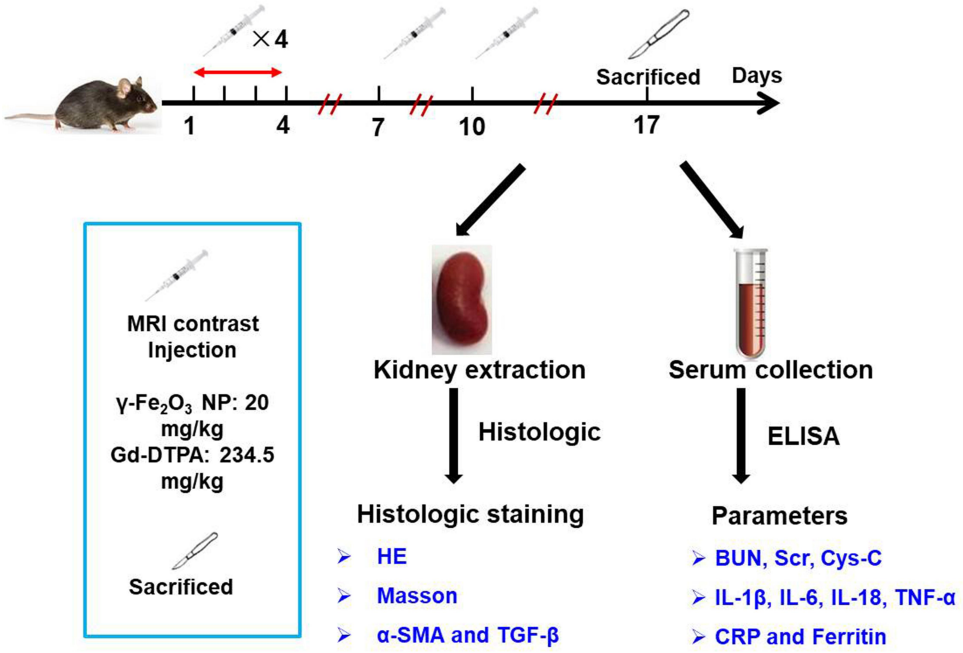

Scheme 1 Illustration for the process and content investigated in this work.

Measurement of Cytotoxicity

Experiments were carried out using the xCELLigence Real-Time Cell Analysis (RTCA) S16 Instrument (ACEA Biosciences, USA) which was placed into an incubator at 37 °C with 5% CO_2. Cell cytotoxicity experiments were performed using gold microelectrodes embedded 16-well plates (E-plate 16 PET, ACEA Biosciences, USA). Cells were seeded at a density of 1×10^4 cells/well for HUVEC. The impedance was recorded at 15 min intervals. Different concentrations of nanomaterials were added to the culture at 5 h and recorded for 96 h.

Animal Experiments

Female Balb/c mice of 6-week old were maintained at the Experimental Animal Center at the Institute of Basic Medical Sciences, Chinese Academy of Medical Sciences (Beijing, China) under specific pathogen-free conditions. Mice were feed in temperature-controlled animal room on a 12: 12-h light dark cycle. All the mice had unlimited access to a standard commercial laboratory diet. All the mice were feed in sterile animal room for one week before the experiment. Animal experiments were carried out and approved in compliance with the regulations of Chinese Academy of Medical Sciences Standing Committee on animal experiments. On the first day, all the mice in the stratified according to body weight and then randomly allocated into groups, including control (saline), γ-Fe_2O_3 NP and Gd-DTPA group (n = 3). The dose of γ-Fe_2O_3 NP was 20 mg/kg per mouse (4 mg/mL), and the dose of Gd-DTPA was 234.5 mg/kg per mouse (46.9 mg/mL). The contrast agents were given on day 1–4, 7 and 10. All the agents were dissolved in saline. The administration volume for each injection was 100 μL.

Sample Collection and Analysis

On Day 17 post the first injection, mice were sacrificed. Serum samples were collected by centrifugation at 4 °C. Blood urea nitrogen (BUN), serum creatinine (Scr), cystatin-c (Cys-C), C-reactive protein (CRP) and ferritin were determined by using a biochemical automatic analyzer (AU5800, Beckman Coulter, USA). The serum level of IL-6, IL-1β and TNF-α was determined by using a mouse multi-factor detection kit (MCYTOMAG-70, Merck Millipore). IL-18 was measured using mouse ELISA kit (EMC011, eBioscience).

Histopathological and Immunohistochemistry Analysis

Kidneys of the mice were harvested, weighed and fixed in 10% neutral-buffered formalin. Paraffinated sections were stained with hematoxylin and eosin (HE) and Masson's trichrome stain (BA-4079A, BASO, China).

Tumor necrosis factor alpha (TNF-α) and transforming growth factor-β (TGF-β) staining were also performed by immunohistochemical analysis. Briefly, the slides were deparaffinized and antigen retrieval was then performed using a microwave oven in EDTA, pH = 8.0 (Servicebio, Wuhan, China). Primary antibodies of TNF-α (1: 300, ab92486, Abcam), TGF-β (1: 200, 19245T, CST, Cambridge, UK) and α-smooth muscle actin (α-SMA) (1: 200, ab5694, Abcam) were incubated overnight before HRP-labeled Goat Anti-Rabbit IgG (H+L) (PV-6001, Beijing Zhongshan Biotechnology) incubation for 50 min at room temperature. Pictures were taken by Nanozoomer (Hamamatsu, Japan). Renal histological analysis was assessed semi-quantitatively by two pathologists with more than 10 years' clinical experience, who was blinded to treatment groups and scored the samples on a scale of 0–5 (0, normal histology; 1, slight injury; 2, mild injury; 3, moderate injury; 4, severe injury).

Statistics

All the experiments were repeated at least three times unless otherwise stated, and the quantitative data are expressed as mean ± standard deviation (SD). Statistical significance was ascertained using the SPSS software (SPPS 20.0) and indicated in the corresponding figure legends. As presented in the figures, p-values below 0.05 were considered to be statistically significant.

Results

Characterizations of MRI Contrast Agents

In this study, two MRI contrast agents were investigated. The molecular formula of Gd-DTPA was provided in Figure 1A. For the γ-Fe_2O_3 NP, Fe atom was detected in the EDX measurement (Figure 1B) and the inserts showed the transmission electron microscopy (TEM) image of γ-Fe_2O_3 NP with the crystal core about 10 nm in diameter.

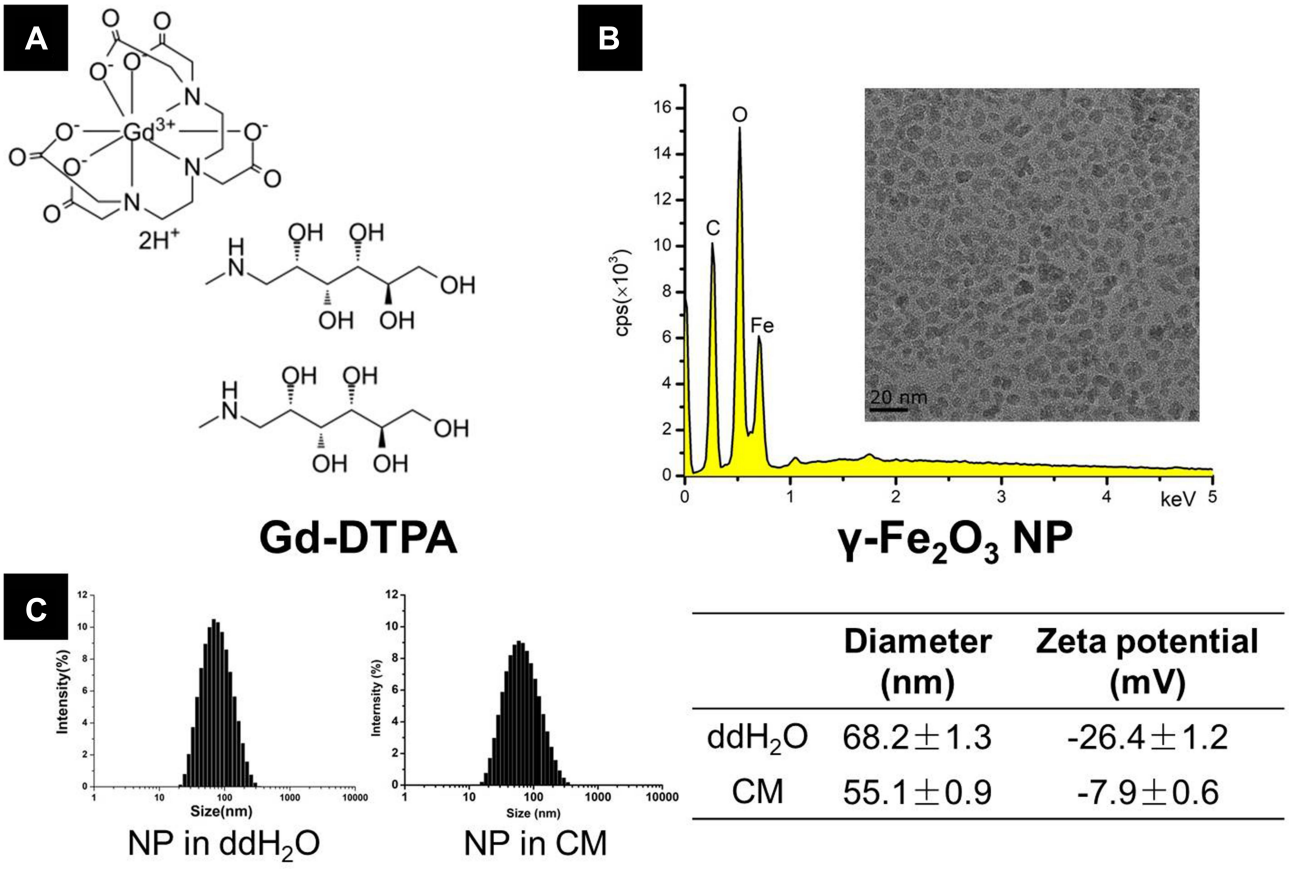

	Diameter (nm)	Zeta potential (mV)
ddH_2O	68.2±1.3	-26.4±1.2
CM	55.1±0.9	-7.9±0.6

Figure 1 (**A**) The formula of Gd-DTPA, (**B**) energy-dispersive X-ray (EDX) images for γ-Fe_2O_3 NP. The insert shows the transmission electron microscopy (TEM) images, and (**C**) dynamic light scattering (DLS) size and zeta potential measurements of γ-Fe_2O_3 NP in ddH_2O and culture medium (CM).

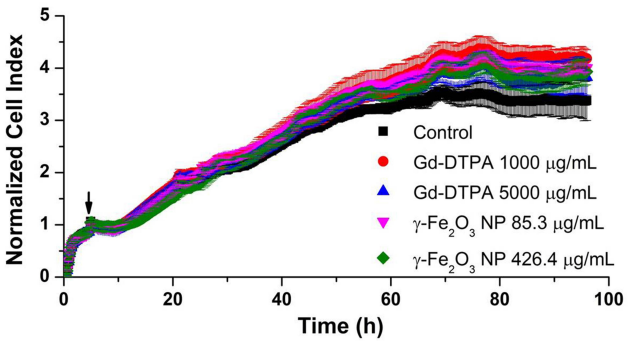

Figure 2 The growth curves of HUVEC cells in the presence of Gd-DTPA or γ-Fe_2O_3 NP at different concentrations. The black arrow indicates the time of the application of contrast agents. Error bars are standard deviation of 3 parallels.

Results obtained from the dynamic light scattering (DLS) exhibited a narrow size distribution of particle diameter both in ddH_2O and in the CM, and the average hydrodynamic diameter of γ-Fe_2O_3 NP was 68.2 ± 1.3 nm and 55.1 ± 0.9 nm in ddH_2O and the CM, respectively. The Zeta potential of γ-Fe_2O_3 NP was -26.4 ± 1.2 mV in ddH_2O to -7.9 ± 0.6 mV in the CM (Figure 1C), the decrease of the negative charge was attributable to the protein adsorption occurring in the CM.

Cell Viability of Human Umbilical Vein Endothelial Cells (HUVEC) in High Dose of Contrast Agents

Firstly, to evaluate the cytotoxicity of these two contrast agents in vitro, the growth curves of HUVEC exposed to high dose of Gd-DTPA or γ-Fe_2O_3 NP were measured by RTCA. The dimensionless parameter (cell index) corresponding to the relative change in measured electrical impedance represents cell status (number of attached

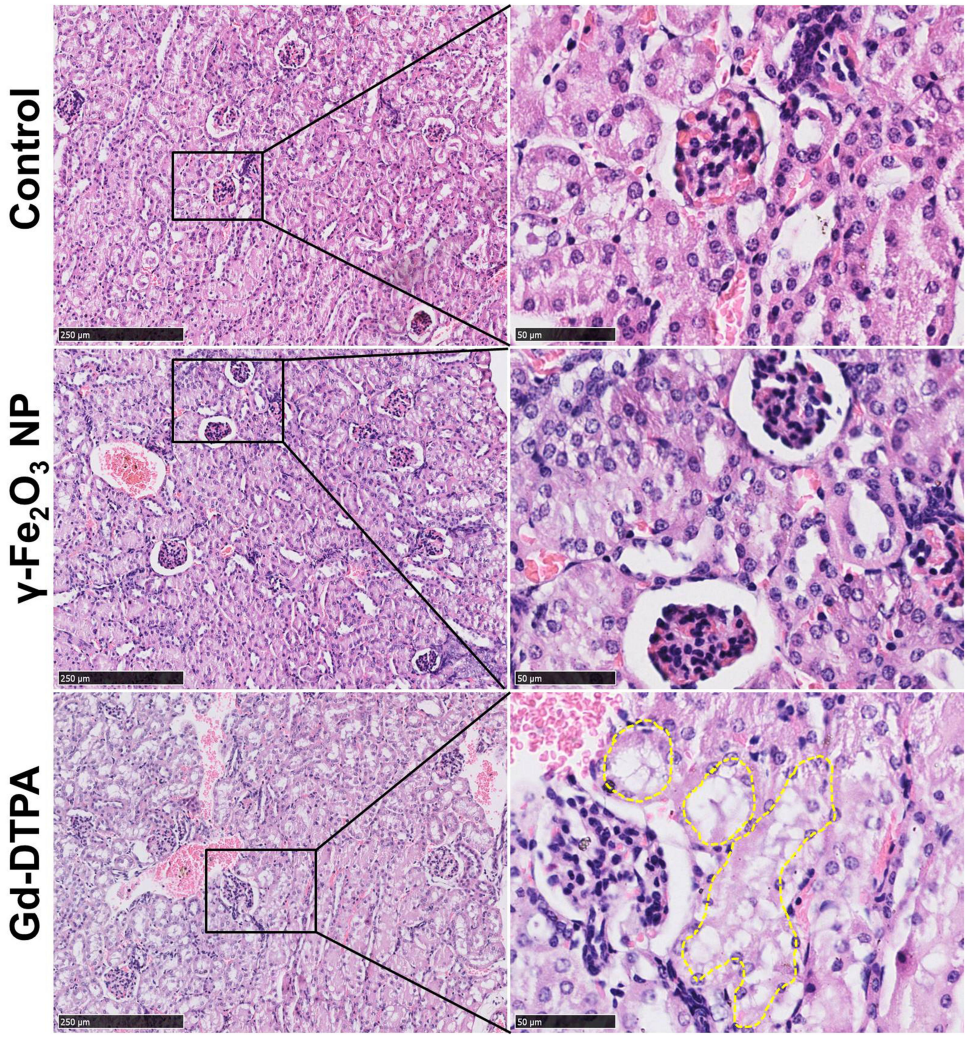

Figure 3 Histopathological images of kidney tissue staining with HE. The right collum was the magnified area of the rectangle box in left collum. Scale bar in left is 250 μm, and scale bar in right is 50 μm. The dot lines circled some typical cytoplasmic vacuoles.

cells) in RTCA system.[29] The values obtained from RTCA system indicated that these two contrast agent observed no significant difference of cytotoxicity over a long incubation time of 96 h (Figure 2).

Histopathological Images of Kidney

The effects in vivo were investigated on female balb/c mice of 6-weeks old, the doses of the contrast agents were equivalent to five times of the dose of clinical routine prescription (1–7 mg/Kg for γ-Fe_2O_3 and 46.9 mg/Kg for Gd-DTPA).[30,31] Histological analysis with the renal tissues of mice was performed with different specific histochemistry staining after 7 days of the last administration. When stained with HE, there were a large number of cytoplasmic vacuoles observed in the renal tubular cells of Gd-DTPA group. By statistically counting the cytoplasmic vacuoles in 10 fields of vision, we showed that there were 45, 48, and 126 cytoplasmic vacuoles in the control, γ-Fe_2O_3 NP and Gd-DTPA group respectively. This indicated the occurrence of kidney injury resulted from the injection of Gd-DTPA, while few cytoplasmic vacuoles were observed in the control group and γ-Fe_2O_3 NP group (Figure 3).

Because organ injury usually leads to the tissue fibrosis and chronic organ dysfunction,[32] the kidney tissue samples from different groups were stained with Masson to examine whether the tissue fibrosis occurred. It was shown that the tissue was darker stained with Masson staining in the Gd-DTPA group, the area was pointed with yellow arrow heads in Figure 4. Differently, there was only a small amount of the area stained in blue in the γ-Fe_2O_3 NP group, not showing significant difference when compared with that in the control group. These indicated that the

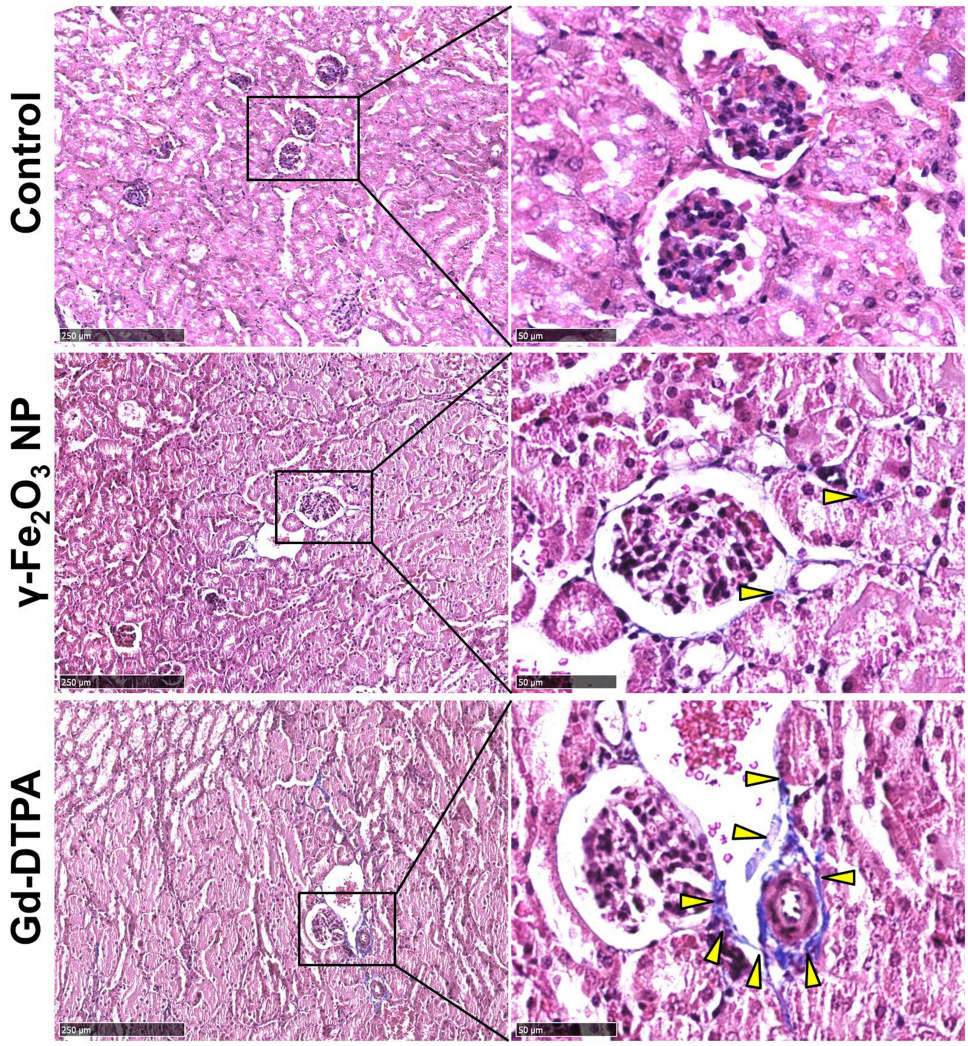

Figure 4 Histopathological images of the kidney tissue stained with Masson. The right collum was the magnified area in the rectangle box in the left collum. Scale bar in left is 250 μm, and scale bar in right is 50 μm. The arrow heads pointed the pathological changes in the tissues.

administration of Gd-DTPA induced the clear signs of tissue fibrosis. We next verified the tissue fibrosis by using anti-mice α-SMA antibody (Figure 5) and anti-mice TGF-β antibody upon the kidney tissues (Figure 6). Results showed that the tissues of Gd-DTPA group exhibited stronger brown stains than that of the other two groups, indicating the occurrence of fibrosis; while no significant difference was observed in the control group and γ-Fe_2O_3 NP group. The statistical analysis result for the histology on the renal was summarized in Table 1, which was performed by two experienced pathologist semi-quantitatively. The staining images and histochemistry statics analysis consistently showed that the administration of Gd-DTPA induced significant kidney injury, while that of γ-Fe_2O_3 NP did not.

Biochemical and Inflammation Factors Measurement

The renal function related biochemical parameters and inflammation factors were measurement by using the biochemical automatic analyzer, multi-factor detection and ELISA kits. The biochemical parameters in renal function include BUN, serum creatinine (Scr) and cystatin C (Cys-C). Results showed that the administration of the two contrast agents did not affect the level of BUN compared with the control. The level of Scr and Cys-C was significantly increased in the Gd-DTPA group while not changed in the γ-Fe_2O_3 NP group when compared with that in the control group (Figure 7). These two are accurate indicators of the kidney function and sensitive to the kidney injury,[33,34] therefore, these results strongly suggested that

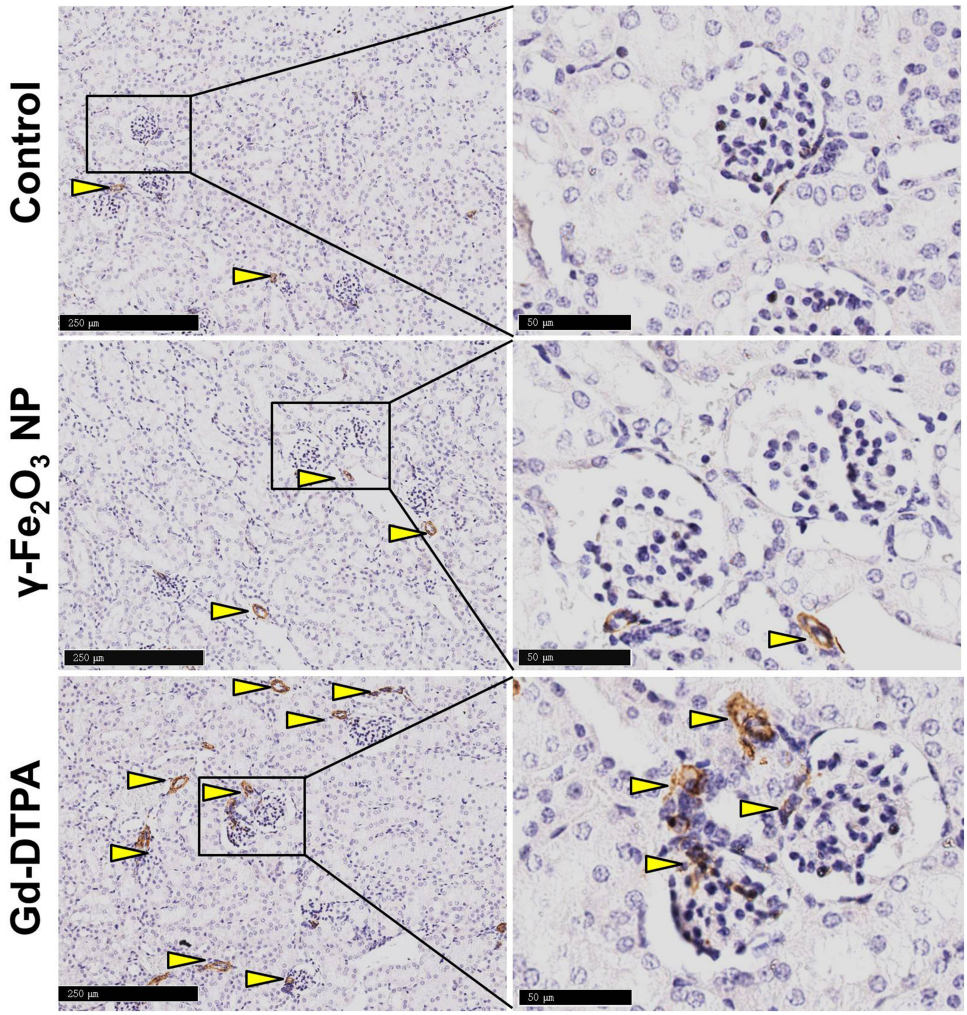

Figure 5 Histological images of kidney tissue staining with α-SMA. The right collum was the magnified area in the rectangle in the left collum. The scale bar is 250 μm in the left and 50 μm in the right. The arrow heads pointed the typical pathological changes in the tissue.

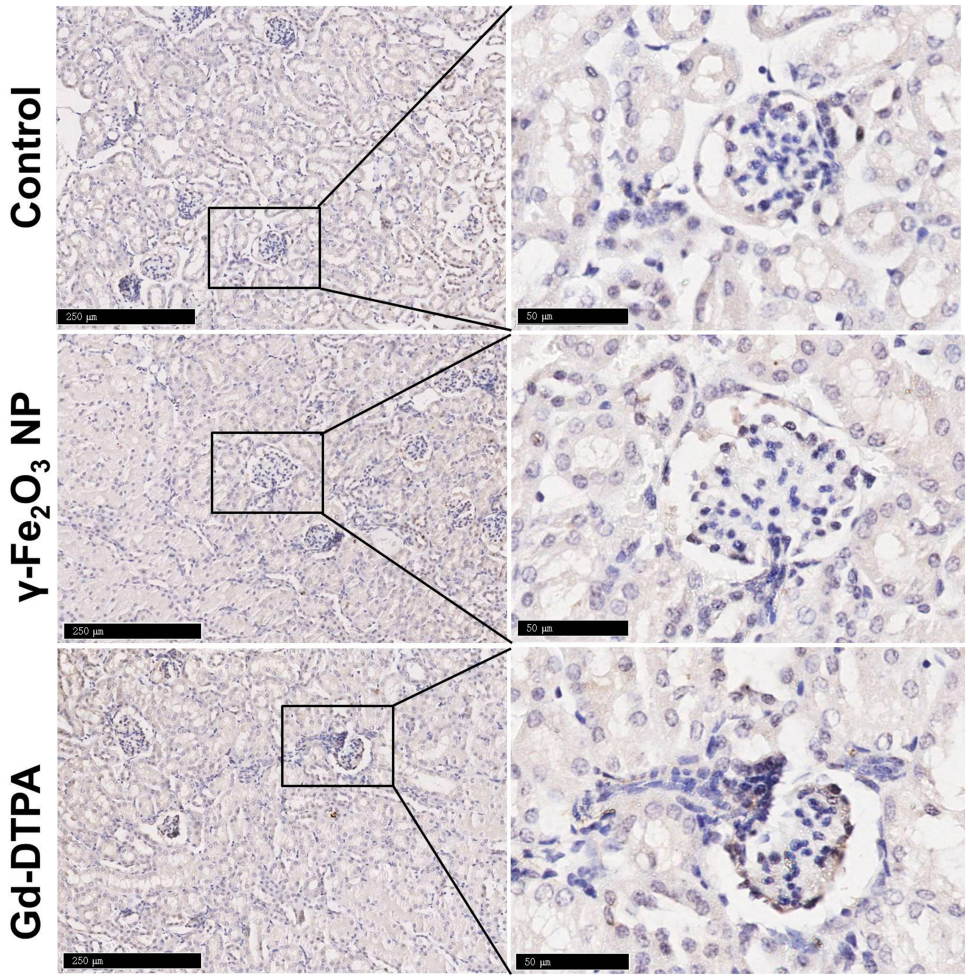

Figure 6 Histological images of kidney tissue staining with TGF-β. The right collum was magnified area in the rectangle in the left collum. The scale bar is 250 μm in the left and 50 μm in the right.

the multiple administration at the high doses of Gd-DTPA was able to cause mild to moderate kidney injury in the healthy mice. With the same injection regime, γ-Fe_2O_3 NP did not affect the renal function. These results were consistent with the histopathological observations.

The inflammation factors are commonly used to indicate the occurrence of acute inflammation. Here we examined IL-1β, IL-6, IL-18, TNF-α, and ferritin by using ELISA kits, and CRP in the blood by biochemical automatic analyzer, all of which are the most common inflammation factor in clinic.[35,36] It was shown that the Gd-DTPA group elicited the highest level of the inflammation factors (IL-1β, IL-6, IL-18, TNF-α, and ferritin). The level of IL-1β in γ-Fe_2O_3 NP group was lower than Gd-DTPA group, although it was also increased compared with the control group. There was no difference detected between the control and γ-Fe_2O_3 NP group for the other inflammation factors (IL-6, IL-18, TNF-α, and ferritin) (Figures 8 and 9). At the same time, Gd-DTPA group showed the highest CRP level (Figure 9), though the differences were not significant in the groups. These results suggested that the administration of γ-Fe_2O_3 NP induced clearly weaker inflammatory responses than that of Gd-DTPA.

Discussion

In this work, γ-Fe_2O_3 NP was coated with polydextrose sorbitol carboxymethyl ether. The average hydrodynamic diameter of γ-Fe_2O_3 NP was a little different with that in TEM image due to the highly hydrophilic coating which increased the hydrodynamic layer on the surface of NPs. The Zeta potential of γ-Fe_2O_3 NP in ddH_2O was -26.4 ± 1.2 mV, indicating a high dispersing stability. Upon the interaction with proteins in the CM, the size decreased a little and Zeta potential changed to close to that of the

Table 1 Quantitative Analysis on the Histopathological Images

Staining	Group	Score				
		0	1	2	3	4
HE	Control	100%	0	0	0	0
	γ-Fe_2O_3 NP	66.67%	33.33%	0	0	0
	Gd-DTPA	0	100%	0	0	0
Masson	Control	100%	0	0	0	0
	γ-Fe_2O_3 NP	100%	0	0	0	0
	Gd-DTPA	0	0	100%	0	0
α-SMA	Control	100%	0	0	0	0
	γ-Fe_2O_3 NP	66.67%	33.33%	0	0	0
	Gd-DTPA	0	0	100%	0	0
TGF-β	Control	100%	0	0	0	0
	γ-Fe_2O_3 NP	100%	0	0	0	0
	Gd-DTPA	0	100%	0	0	0

Notes: Scores 0, normal histology; 1, slight injury; 2, mild injury; 3, moderate injury; 4, severe injury.

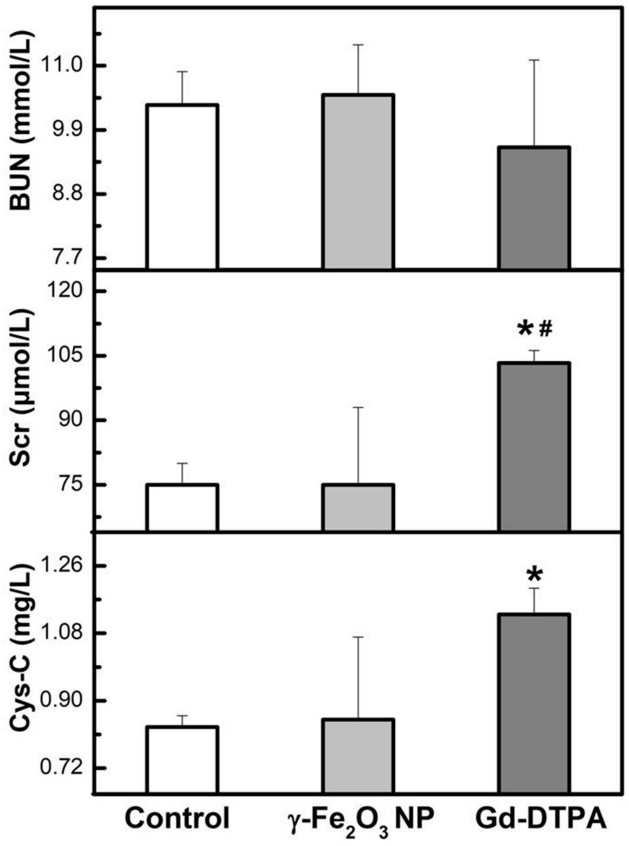

Figure 7 Measurement of the biochemical factors (BUN, Scr and Cys-C) from serum of mice. Data are presented from a representative experiment (mean ± SD, n = 3). Statistical analysis was performed with one-way ANOVA followed by least-significant-difference (LSD) post hoc test for BUN, Scr. Statistical analysis was performed with one-way ANOVA followed by Dunnett-T3 post hoc test for Cys-C. *P < 0.05, compared with control, #P < 0.05 compared with γ-Fe_2O_3 NP group.

pure CM (-6.8 ± 0.5 mV), indicating a dispersing stability in the biological liquids. Here, we have shown that Gd-DTPA was able to cause moderate harmful changes on the kidney even in healthy mice by multiple administrations with the high doses. On the contrary, γ-Fe_2O_3 NP showed a better compatibility than Gd-DTPA from the view of proinflammatory effects. These results indicated that although no significant cytotoxicity was detected with both contrasts in the endothelial cells experiment for a long incubation time, the two contrasts exhibited significantly different effects in vivo, which strongly suggested that in this situation, the conventional cytotoxicity assay cannot well reflect the real situation in vivo. Furthermore, even in the healthy mice, repeated administration of Gd-DTPA could induce kidney injury, tissue fibrosis and inflammation, on the contrary, γ-Fe_2O_3 NP did not cause less changes.

It has been recognized that NP only less than 6 nm in diameter are able to go renal clearance, and 30–99% of administered NP will accumulate and sequester in the liver after administration into the body.[37] Given the average diameter of 68.2 ± 1.3 nm, γ-Fe_2O_3 NPs were likely go through hepatobiliary excretion pathway and may interact with hepatic cells. This is the reason its lower kidney toxicity was exhibited in reference to that of GBCAs. On the other hands, this feature may bring potential risk in liver. In our previous investigations, the γ-Fe_2O_3 NPs were observed in the liver tissue of mice receiving the intravenous injection once a day for 7 days with the same high dose of this work.[38] We found out that the injection up regulated the expression of CD31 and α-SMA in the liver, indicating an oxidative stress occurred, and which could be rescued by the use of reactive oxygen species scavenger mannitol or ascorbic acid. In addition, iron oxide-based nanomaterials were reported to undergo slow degradation in Kupffer cells and become sequestered in the mononuclear phagocyte system organs in the non-toxic form.[39,40] From above aspects, it is possible to take prevention and treatment to overcome the limitation in clinic applications.

For patients, many factors were able to cause kidney damage, regardless the disease itself, ages, hypertension, diabetes, and drugs or ways to treat the disease were involved. Due to above reasons, chronic kidney diseases are highly prevalent in all over the world and most of them were silent and unknown without obvious indicators.[41] This may explain that serious side effects of Gd-DTPA could happen sometimes in certain patients with "healthy"

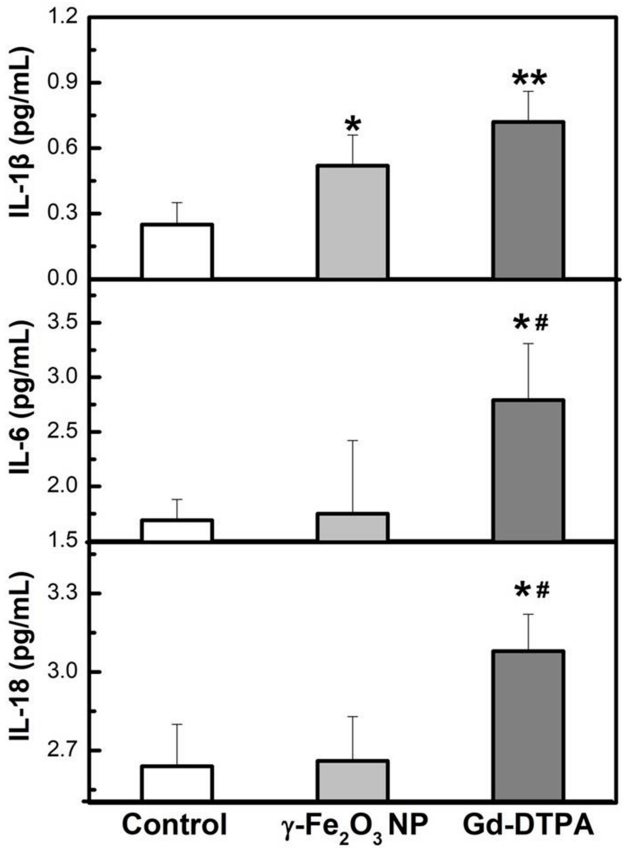

Figure 8 Measurement of the cytokines factors (IL-1β, IL-6, IL-18) from serum of mice. Data are presented from a representative experiment (mean ± SD, n = 3). Statistical analysis was performed with one-way ANOVA followed by least-significant-difference (LSD) post hoc test *P < 0.05, **P < 0.01 compared with control, #P < 0.05 compared with γ-Fe_2O_3 NP group.

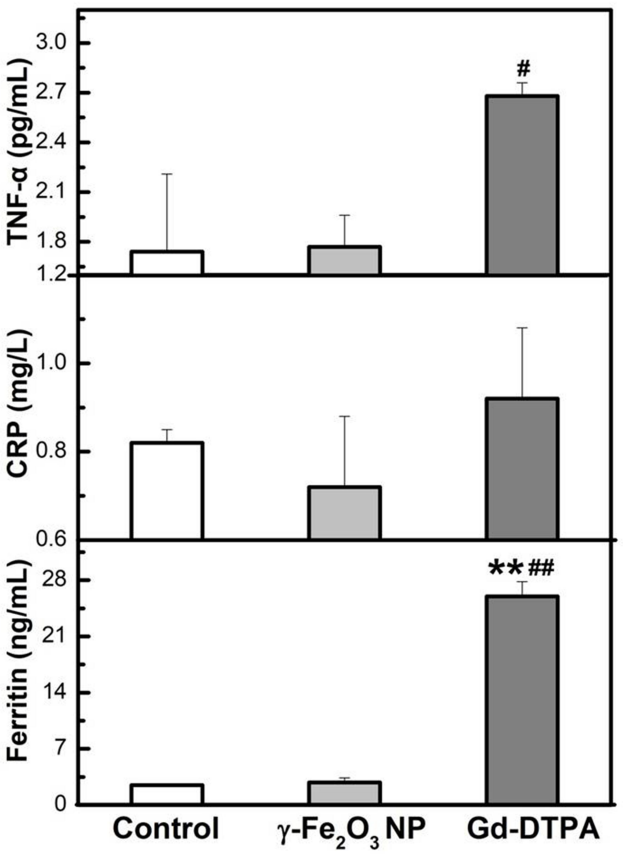

Figure 9 Measurement of TNF-α, CRP and Ferritin from serum of mice. Data are presented from a representative experiment (mean ± SD, n = 3). Statistical analysis was performed with one-way ANOVA followed by least-significant-difference (LSD) post hoc test for CRP. Statistical analysis was performed with one-way ANOVA followed by Dunnett-T3 post hoc test for TNF-α and Ferritin. **P < 0.01, compared with control, #P < 0.05, ##P < 0.01 compared with γ-Fe_2O_3 NP group.

kidney.[26,42] Given above circumstances, if any potential kidney injury risk factors are pre-existed, the patients even with normal kidney function should be not given Gd-DTPA as MRI imaging contrast. Therefore, when repeated MRI enhancement imaging scanning was required for one patient, such as cancer and vascular disease with multi-lesions, γ-Fe_2O_3 NP should be a safer and important option of MRI contrast by clinicians. Due to the possible potential toxicity in the liver, prevention and treatment can be taken to overcome this possible limitation in clinic applications.

Conclusion

In summary, when administrated repeatedly with high doses, Gd-DTPA could induce moderate kidney injury through eliciting inflammatory effects leading to the fibrosis while γ-Fe_2O_3 NP did not induce obvious difference compared with the control group. It is important for both healthcare practitioners and patients to avoid side effects and following problems of each measure as far as possible during the diagnosis, and the results in this study provided an extremely important hint for clinicians.

Ethics Approval

This study was performed in accordance with the regulations of Chinese Academy of Medical Sciences Standing Committee on animal experiments and was approved by the Institutional Animal Care and Use committee (Institute of Basic Medical Sciences, Chinese Academy of Medical Sciences, and Peking Union Medical College, Beijing, China).

Acknowledgments

This work was supported by the National Key R&D Program of China (2017YFA0205504), National Natural Science Foundation of China (81801771), and CAMS Innovation Fund for Medical Sciences (CIFMS 2016-I2M-3-004).

Author Contributions

All authors contributed to data analysis, drafting or revising the article, have agreed on the journal to which the article will be submitted, gave final approval of the version to be published, and agree to be accountable for all aspects of the work.

Disclosure

The authors report no conflicts of interest in this work.

References

1. Biegger P, Ladd ME, Komljenovic D. Multifunctional magnetic resonance imaging probes. *Recent Results Cancer Res*. 2020;216:189–226.
2. Fraum TJ, Ludwig DR, Bashir MR, Fowler KJ. Gadolinium-based contrast agents: a comprehensive risk assessment. *J Magn Reson Imaging*. 2017;46(2):338–353. doi:10.1002/jmri.25625
3. Rudnick MR, Wahba IM, Leonberg-Yoo AK, Miskulin D, Litt HI. Risks and options with gadolinium-based contrast agents in patients with CKD: a review. *Am J Kidney Dis*. 2020;S0272–6386(20):30926.
4. Todd DJ, Kay J. Gadolinium-induced fibrosis. *Annu Rev Med*. 2016;67:273–291. doi:10.1146/annurev-med-063014-124936
5. Wei H, Bruns OT, Kaul MG, et al. Exceedingly small iron oxide nanoparticles as positive MRI contrast agents. *Proc Natl Acad Sci U S A*. 2017;114(9):2325–2330. doi:10.1073/pnas.1620145114
6. Avasthi A, Caro C, Pozo-Torres E, Leal MP, García-Martín ML. Magnetic nanoparticles as MRI contrast agents. *Top Curr Chem*. 2020;378(3):40.
7. Deng L-H, Jiang H, Lu F-L, et al. Size and PEG length-controlled PEGylated monocrystalline superparamagnetic iron oxide nanocomposite for MRI contrast agent. *Int J Nanomed*. 2021;16:201–211. doi:10.2147/IJN.S271461
8. Cai X, Zhu Q, Zeng Y, Zeng Q, Chen X, Zhan Y. Manganese oxide nanoparticles as MRI contrast agents in tumor multimodal imaging and therapy. *Int J Nanomed*. 2019;Volume 14(14):8321–8344. doi:10.2147/IJN.S218085
9. Cardoso VF, Francesko A, Ribeiro C, Banobre-Lopez M, Martins P, Lanceros-Mendez S. Advances in magnetic nanoparticles for biomedical applications. *Adv Healthc Mater*. 2018;7(5):1700845.
10. Hu Y, Mignani S, Majoral JP, Shen M, Shi X. Construction of iron oxide nanoparticle-based hybrid platforms for tumor imaging and therapy. *Chem Soc Rev*. 2018;47(5):1874–1900. doi:10.1039/C7CS00657H
11. Zhao S, Yu X, Qian Y, Chen W, Shen J. Multifunctional magnetic iron oxide nanoparticles: an advanced platform for cancer theranostics. *Theranostics*. 2020;10(14):6278–6309. doi:10.7150/thno.42564
12. Zhi D, Yang T, Yang J, Fu S, Zhang S. Targeting strategies for superparamagnetic iron oxide nanoparticles in cancer therapy. *Acta Biomater*. 2020;102:13–34. doi:10.1016/j.actbio.2019.11.027
13. Xiao Y, Du J. Superparamagnetic nanoparticles for biomedical applications. *J Mater Chem B*. 2020;8(3):354–367. doi:10.1039/C9TB01955C
14. Jahangirian H, Kalantari K, Izadiyan Z, Rafiee-Moghaddam R, Shameli K, Webster TJ. A review of small molecules and drug delivery applications using gold and iron nanoparticles. *Int J Nanomedicine*. 2019;14:1633–1657. doi:10.2147/IJN.S184723
15. Wáng YXJ, Idée J-M. A comprehensive literatures update of clinical researches of superparamagnetic resonance iron oxide nanoparticles for magnetic resonance imaging. *Quant Imaging Med Surg*. 2017;7(1):88–122. doi:10.21037/qims.2017.02.09
16. Bao Y, Sherwood JA, Sun Z. Magnetic iron oxide nanoparticles as T1 contrast agents for magnetic resonance imaging. *J Mater Chem C*. 2018;6(6):1280–1290. doi:10.1039/C7TC05854C
17. Azria D, Blanquer S, Verdier J-M, Belamie E. Nanoparticles as contrast agents for brain nuclear magnetic resonance imaging in Alzheimer's disease diagnosis. *J Mater Chem B*. 2017;5(35):7216–7237.
18. Wang Y-XJ. Superparamagnetic iron oxide based MRI contrast agents: current status of clinical application. *Quant Imaging Med Surg*. 2011;1(1):35–40. doi:10.3978/j.issn.2223-4292.2011.08.03
19. Frtús A, Smolková B, Uzhytchak M, et al. Analyzing the mechanisms of iron oxide nanoparticles interactions with cells: a road from failure to success in clinical applications. *J Controlled Release*. 2020;328:59–77. doi:10.1016/j.jconrel.2020.08.036
20. FDA. Drug safety and availability - FDA drug safety communication. Available from: https://www.fda.gov/drugs/drug-safety-and-availability/fda-drug-safety-communication-fda-strengthens-warnings-and-changes-prescribing-instructions-decrease. Accessed March 30, 2015.
21. Nguyen K-L, Yoshida T, Kathuria-Prakash N, et al. Multicenter safety and practice for off-label diagnostic use of ferumoxytol in MRI. *Radiology*. 2019;293:554–564. doi:10.1148/radiol.2019190477
22. Chen R, Ling D, Zhao L, et al. Parallel comparative studies on mouse toxicity of oxide nanoparticle- and gadolinium-based T1 MRI contrast agents. *ACS Nano*. 2015;9(12):12425–12435. doi:10.1021/acsnano.5b05783
23. Weng Q, Hu X, Zheng J, et al. Toxicological risk assessments of iron oxide nanocluster- and gadolinium-based T1 MRI contrast agents in renal failure rats. *ACS Nano*. 2019;13(6):6801–6812. doi:10.1021/acsnano.9b01511
24. Frenzel T, Apte C, Jost G, Schockel L, Lohrke J, Pietsch H. Quantification and assessment of the chemical form of residual gadolinium in the brain after repeated administration of gadolinium-based contrast agents: comparative study in rats. *Invest Radiol*. 2017;52(7):396–404. doi:10.1097/RLI.0000000000000352
25. Kanda T, Oba H, Toyoda K, Kitajima K, Furui S. Brain gadolinium deposition after administration of gadolinium-based contrast agents. *Jpn J Radiol*. 2016;34(1):3–9. doi:10.1007/s11604-015-0503-5
26. Roberts DR, Lindhorst SM, Welsh CT, et al. High levels of gadolinium deposition in the skin of a patient with normal renal function. *Invest Radiol*. 2016;51(5):280–289. doi:10.1097/RLI.0000000000000266
27. Mathur M, Jones JR, Weinreb JC. Gadolinium deposition and nephrogenic systemic fibrosis: a radiologist's primer. *Radiographics*. 2020;40(1):153–162. doi:10.1148/rg.2020190110
28. Chen B, Li Y, Zhang X, et al. An efficient synthesis of ferumoxytol induced by alternating-current magnetic field. *Mater Lett*. 2016;170:93–96. doi:10.1016/j.matlet.2016.02.006
29. Oberg HH, Peters C, Kabelitz D, Wesch D. Real-time cell analysis (RTCA) to measure killer cell activity against adherent tumor cells in vitro. *Methods Enzymol*. 2020;631:429–441.
30. Bose C, Megyesi JK, Shah SV, et al. Evidence suggesting a role of iron in a mouse model of nephrogenic systemic fibrosis. *PLoS One*. 2015;10(8):e0136563. doi:10.1371/journal.pone.0136563
31. Toth GB, Varallyay CG, Horvath A, et al. Current and potential imaging applications of ferumoxytol for magnetic resonance imaging. *Kidney Int*. 2017;92(1):47–66. doi:10.1016/j.kint.2016.12.037
32. Mack M. Inflammation and fibrosis. *Matrix Biol*. 2018;68–69:106–121.
33. Ronco C, Bellomo R, Kellum JA. Acute kidney injury. *Lancet*. 2019;394(10212):1949–1964. doi:10.1016/S0140-6736(19)32563-2
34. Bagshaw SM, Bellomo R. Cystatin C in acute kidney injury. *Curr Opin Crit Care*. 2010;16(6):533–539. doi:10.1097/MCC.0b013e32833e8412

35. Prieto-Moure B, Lloris-Carsi JM, Belda-Antoli M, Toledo-Pereyra LH, Cejalvo-Lapena D. Allopurinol protective effect of renal ischemia by downregulating TNF-alpha, IL-1beta, and IL-6 response. *J Invest Surg*. 2017;30(3):143–151. doi:10.1080/08941939.2016.1230658
36. Wu Y, Potempa LA, El Kebir D, Filep JG. C-reactive protein and inflammation: conformational changes affect function. *Biol Chem*. 2015;396(11):1181–1197.
37. Zhang Y-N, Poon W, Tavares AJ, Mc Gilvray ID, Chan WC. Nanoparticle-liver interactions: cellular uptake and hepatobiliary elimination. *J Controlled Release*. 2016;240:332–348. doi:10.1016/j.jconrel.2016.01.020
38. Wen T, Du L, Chen B, et al. Iron oxide nanoparticles induce reversible endothelial-to-mesenchymal transition in vascular endothelial cells at acutely non-cytotoxic concentrations. *Part Fibre Toxicol*. 2019;16(1):30. doi:10.1186/s12989-019-0314-4
39. Jain TK, Reddy MK, Morales MA, Leslie-Pelecky DL, Labhasetwar V. Biodistribution, clearance, and biocompatibility of iron oxide magnetic nanoparticles in rats. *Mol Pharm*. 2008;5(2):316–327. doi:10.1021/mp7001285
40. Levy M, Luciani N, Alloyeau D, et al. Long term in vivo biotransformation of iron oxide nanoparticles. *Biomaterials*. 2011;32(16):3988–3999. doi:10.1016/j.biomaterials.2011.02.031
41. Chen TK, Knicely DH, Grams ME. Chronic kidney disease diagnosis and management: a review. *J Am Med Assoc*. 2019;322(13):1294–1304. doi:10.1001/jama.2019.14745
42. Semelka RC, Commander CW, Jay M, Burke LM, Ramalho M. Presumed gadolinium toxicity in subjects with normal renal function: a report of 4 cases. *Invest Radiol*. 2016;51(10):661–665. doi:10.1097/RLI.0000000000000318